Supporting Information for

Ionophobic nanopore enhancing capacitance and charging dynamics in supercapacitor with ionic liquids

Zhongdong Gan[a,b], Yanlei Wang[b,c,], Mi Wang[b,c], Enlai Gao[e], Feng Huo[b,c], Weilu Ding[b,c], Hongyan He[b,c,d,*] and Suojiang Zhang[a,b,c,*]*

[a]School of Chemical Engineering and Technology, Tianjin University, Tianjin, 300072 China

[b]Beijing Key Laboratory of Ionic Liquids Clean Process, State Key Laboratory of Multiphase Complex Systems, CAS Key Laboratory of Green Process and Engineering, Institute of Process Engineering, Chinese Academy of Sciences, Beijing 100190, China

[c]University of Chinese Academy of Sciences, Beijing 100049, China

[d]Innovation Academy for Green Manufacture, Chinese Academy of Sciences, Beijing 100190, China

[e]Department of Engineering Mechanics, School of Civil Engineering, Wuhan University, Wuhan, Hubei 430072, China

Corresponding Authors:

Email: ylwang17@ipe.ac.cn (Y. Wang); hyhe@ipe.ac.cn (H. He); sjzhang@ipe.ac.cn (S. Zhang)

Supporting Tables:

Table S1. Interface Energy of $EMIMBF_4$-Grapheen with different VDW interactions

η_{ion}	0.3	0.4	0.5	0.6
Γ (J/m^2)	1.678	0.975	-0.052	-0.854
η_{ion}	0.7	1.0	1.2	1.5
Γ (J/m^2)	-1.526	-3.985	-5.636	-8.176

Table S2. Differential Capacitances of computational and experimental results.[1-8]

Electrode material	Electrolyte	Capacitance ($\mu F/cm^2$)	Reference
Planar graphene	[BMIM] [PF_6]	4.8	[1] MD
Graphite	[$C_n$mim] [TFSI]	5.5	[2] MD
3-layer graphene	[pyr_{13}] [TFSI]	4.8	[3] MD
2-layer graphene	[pyr_{13}] [FSI]	5.0	[4] MD
1-layer graphene	[BMIM] [PF_6]	5.0~6.5	[5] exp
5-layer graphene	6M KOH	2.0~4.0	[6] exp
5-layer graphene	[BMIM] [PF_6]	3.0~4.0	[7] exp
3-layer graphene	[BMIM] [BF_4]	5.5	[8] MD
3-layer graphene	[BMIM] [BF_4]	4.9	[8] MD

Supporting Figures and Captions:

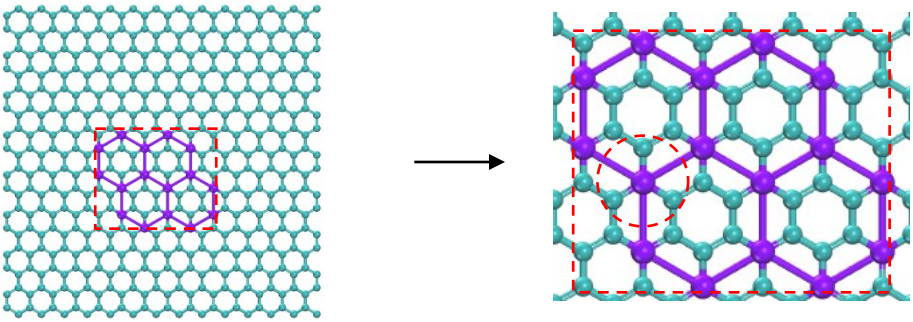

Figure S1. Coarse-grained lattice of graphene. The magnified image shows that each bead in the coarse-grained model represents 4 atoms.

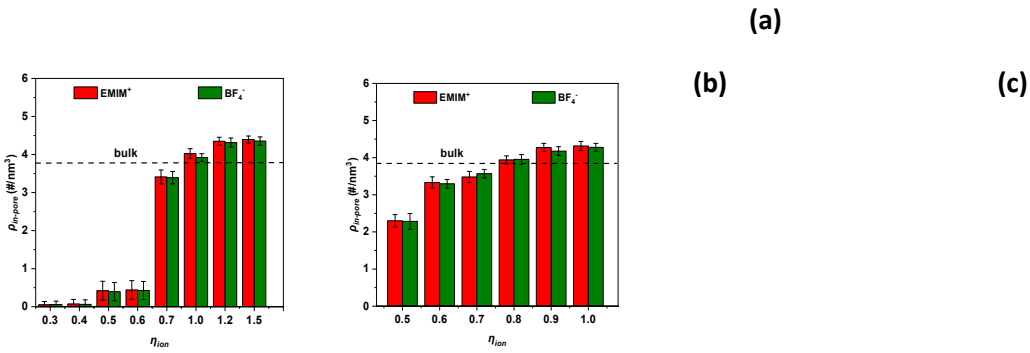

Figure S2. The in-pore ion population at 0 V as a function of the regulated interaction ηion = ε/ε0: (a) 2.46 nm and (b) 3.3 nm. (c) A snapshot of simulation for interface energy calculating. The system consists of a 5-layer graphene base (33.95*33.6 Å) and 130 pairs of EmimBF_4.

Table S3. The specific charge density of different electrodes

U_{ele} (V) \ η_{ion}	0.3	0.5	1.0	1.5
-4.0	-23.7045	-23.0056	-21.5873	-21.8472
-3.5	-20.9756	-20.3887	-19.4409	-19.5904
-3.0	-18.0833	-17.9807	-17.0633	-17.1981
-2.5	-15.0498	-15.1491	-14.5744	-14.3373
-2.0	-12.2647	-12.2089	-11.5392	-11.2671
-1.5	-8.9268	-9.3651	-8.1686	-7.7449
-1.0	-5.4659	-6.2517	-4.9723	-4.9702
-0.5	-2.6005	-2.5982	-2.2153	-2.1523
0.0	0.0000	0.0000	0.0000	0.0000
0.5	2.5999	2.5983	2.2144	2.1538
1.0	5.4662	6.2475	4.9498	4.9768
1.5	8.9279	9.3654	8.1332	7.7509
2.0	12.2654	12.2079	11.5061	11.2678
2.5	15.0534	15.1495	14.5127	14.3386
3.0	18.0871	17.9822	17.0263	17.1994
3.5	20.9817	20.3929	19.4186	19.5912
4.0	23.7110	23.0133	21.6111	21.8573

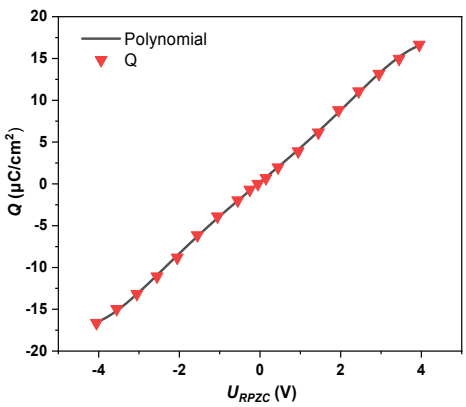

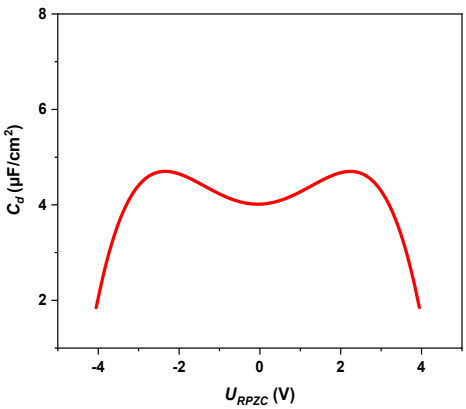

S5

Figure S3. Method to obtain the differential capacitance. (a) The relationship between V_{RPZC} and the electrode surface charge density σ. Points shown as triangles were obtained from simulations, the solid line were the results of the 5-order polynomial fitting. (b) The plot of differential capacitance VS V_{RPZC} obtained from $C_d = dQ/dU_{RPZC}$. The way of obtaining the DC was the same as in several previous work [9, 10]: an order of five polynomial was employed to fit the simulating values of electrode charge density on U_{RPZC} and then the DC was received as the analytical derivative of the fitted polynomial with respect to $U_{RPZC,}$

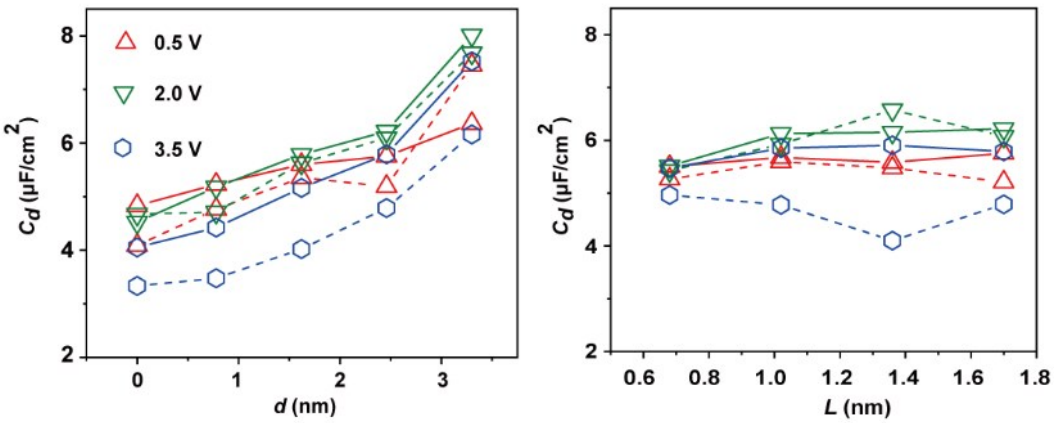

Figure S4. The differential capacitance (U_{RPZC} = 0.5, 2.0, 3.5 V) as a function of the pore size (d) and pore length (L). The solid and dashed lines represent the ionophobic and ionophilic electrode, respectively.

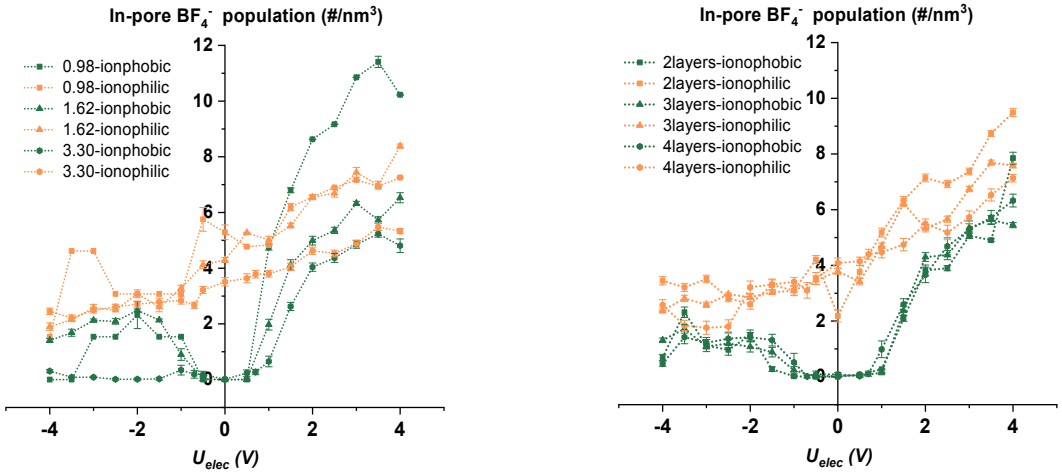

Figure S5. In-pore anion population at different electrodes as a function of the electrical voltage. (a) Porous electrodes with different pore diameters. (b) Porous electrodes with different pore lengths.

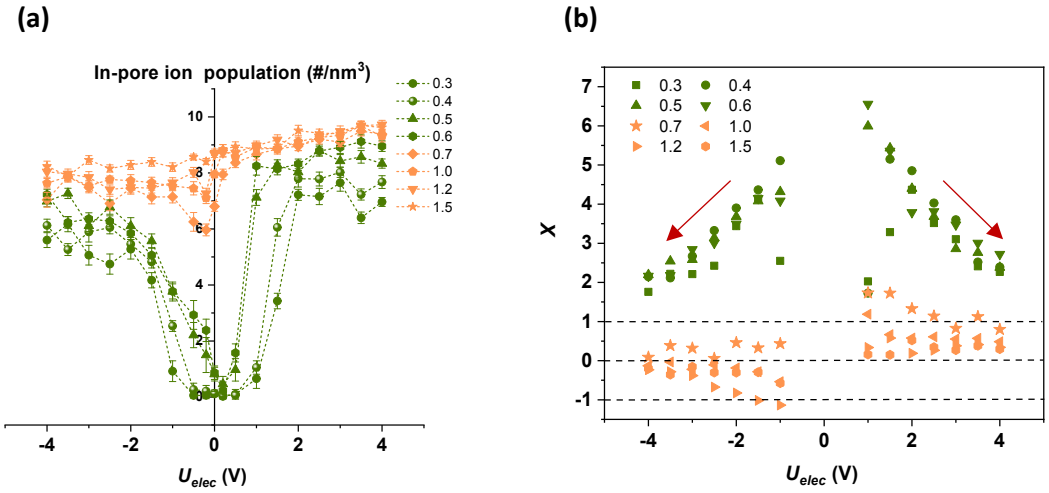

Figure S6. (a) Total number of ions in ionophobic and ionophilic pore at different applied potentials with different coupling strength. (b) Charging mechanism parameters in ionophobic and ionophilic systems at different applied potentials with different coupling strength.

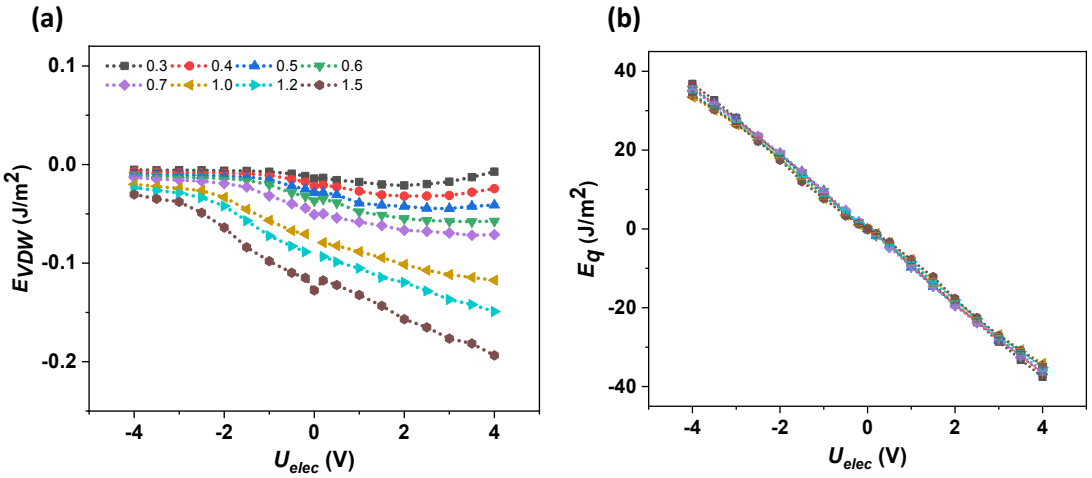

Figure S7. VDW (a) and electrostatic (b) interaction between anion-electrode at different potentials with different coupling strength.

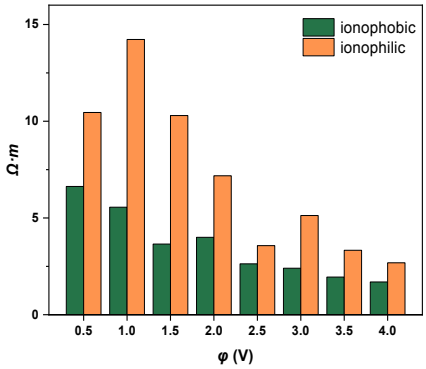

Figure S8. The resistivity of the electrode with ionophobic and ionophilic pore (d_{pore} = 2.46 nm) at different applied potentials.

Supplementary Note S1: Simulation of the equivalent circuit

The resistance of the bulk electrolyte R_{bulk} is derived from the electrical conductivity. First five independent simulations at 298 K were conducted to compute the mean-square displacements (MSDs) and the self-diffusion coefficient was received using the Einstein relation:

$$D_s = \frac{1}{6}\lim_{t\to\infty}\frac{d}{dt}\left\langle \left| r_i(t) - r_i(0) \right|^2 \right\rangle$$

where $r_i(t)$ is the center of mass (COM) position of ion i at time t. Then the conductivity was calculated by Nernst−Einstein (NE) relation:

$$\sigma_{NE} = \frac{N_{pair}}{Vk_BT}(q_+^2 D_+ + q_-^2 D_-)$$

In the equation, N_{pair} is the number of ion pairs, V the simulation box volume, k_B the Boltzmann constant, and T the temperature. q_+ and q_- are the total charges of the ions (full charges were used), and D_+ and D_- are the self-diffusion coefficients of the cations and anions, respectively. From the simulation, D_+ and D_- are 6.66×10^{-11} m^2/s and 3.51×10^{-11} m^2/s In the end we received the σ=2.418 S m^{-1} and the bulk resistance is $7.25\times10^7\Omega$.

Here we present the analytical results for the charging of the equivalent circuit described in Figure 4 of the manuscript, which are used to analyze the molecular simulation data. From the impedance associated with each component, namely R_{bulk}, R_1, R_2, $1/jC_1\omega$ and $1/jC_2\omega$, and their combination in series and in parallel, the overall impedance of the simulation cell is easily derived as:

$$Z(\omega) = \frac{(j\omega)^2 R_2(R_{bulk}+2R_1)C_1C_2 + j\omega[(R_{bulk}+2R_1)C_1 + (R_{bulk}+2R_1+2R_2)C_2] + 2}{(j\omega)^2 R_2C_1C_2 + j\omega(C_1+C_2)}$$

In Fourier space, the total charge Q of the electrodes is related to the voltage V as:

$$Q(\omega)=\frac{I(\omega)}{j\omega}=\frac{V(\omega)}{j\omega Z(\omega)}$$

where $I(\omega)$ is the intensity.

$$\left[(j\omega)^2+j\omega a+b\right]Q(\omega)=[c+j\omega a]V(\omega)$$

In this equation, the expressions of constants are:

$$a=\frac{(R_{bulk}+2R_1)C_1+(R_{bulk}+2R_1+2R_2)C_2}{R_2(R_{bulk}+2R_1)C_1C_2}$$

$$b=\frac{2}{R_2(R_{bulk}+2R_1)C_1C_2}$$

$$c=\frac{C_1+C_2}{R_2(R_{bulk}+2R_1)C_1C_2}$$

$$d=\frac{1}{R_{bulk}+2R_1}$$

As a result, the total charge *Q*(t) satisfies the following differential equation:

$$Q''(t)+aQ'(t)+bQ(t)=cV(t)+dV'(t)$$

with the same constants *a*, *b*, *c*, *d*. Based on ref [on the dynamics], the solution finally comes to the expression as the manuscript:

$$Q(t)=Q_{max}[1-A_1\exp(-\frac{t}{\tau_1})-A_2\exp(-\frac{t}{\tau_2})]$$

with the following constants:

$$Q_{max}=\frac{c}{b}V_0=\frac{C_1+C_2}{2}V_0$$

$$\tau_1=\frac{2}{a+\sqrt{a^2-4b}}$$

$$\tau_2=\frac{2}{a-\sqrt{a^2-4b}}$$

$$A_1 = \frac{1}{2}[1 + \frac{2bd - ac}{2c\sqrt{a^2 - 4b}}]$$

$$A_2 = \frac{1}{2}[1 - \frac{2bd - ac}{2c\sqrt{a^2 - 4b}}]$$

The charges Q_1 and Q_2 of both slices of the electrode can also be determined from the impedance of each branch of the circuit. The solution for Q_1(t) is then obtained by replacing these coefficients in the solution for Q(t).

Supporting References:

1. E. Paek, A. J. Pak and G. S. Hwang, *J. Electrochem. Soc.*, 2012, **160**, A1-A10.
2. J. Vatamanu, O. Borodin, D. Bedrov and G. D. Smith, *J. Phys. Chem. C*, 2012, **116**, 7940-7951.
3. J. Vatamanu, O. Borodin and G. D. Smith, *J. Am. Chem. Soc.*, 2010, **132**, 14825-14833.
4. J. Vatamanu, O. Borodin and G. D. Smith, *J. Phys. Chem. B*, 2011, **115**, 3073-3084.
5. J. Xia, F. Chen, J. Li and N. Tao, *Nat. Nanotechnol.*, 2009, **4**, 505-509.
6. H. Ji, X. Zhao, Z. Qiao, J. Jung, Y. Zhu, Y. Lu, L. L. Zhang, A. H. MacDonald and R. S. Ruoff, *Nat. Commun.*, 2014, **5**, 3317.
7. E. Uesugi, H. Goto, R. Eguchi, A. Fujiwara and Y. Kubozono, *Sci Rep*, 2013, **3**, 1595.
8. C. Merlet, M. Salanne and B. Rotenberg, *J. Phys. Chem. C*, 2012, **116**, 7687-7693.
9. M. Sha, Q. Dou, F. Luo, G. Zhu and G. Wu, *ACS Appl. Mater. Interfaces*, 2014, **6**, 12556-12565.
10. N. Georgi, A. A. Kornyshev and M. V. Fedorov, *J. Electroanal. Chem.*, 2010, **649**, 261-267.